Chronic Pain and Management Journal
Pomakidou S, et al. Chron Pain Manag 8: 165.
www.doi.org/10.29011/2576-957X.100065
www.gavinpublishers.com

Research Article

# Wearable Motion Analysis in Sports: Advancing Biomechanical Insights Beyond the Laboratory

**Sofia Pomakidou[1], Christos Marmarinos[2], Stella Agrotou[2], Athanasios Moustogiannis[3*], Alexandros Nikolopoulos[2], Nikolaos Kostopoulos[2]**

[1]CEO Evo 4 Human Performance, Greece

[2]School of Physical Education and Sport Science, National and Kapodistrian University of Athens, Athens, Greece

[3]Department of Sports Science, New York College, Athens, Greece

[*]**Corresponding author:** Athanasios Moustogiannis, Department of Sports Science, New York College, Athens, Greece

**Citation:** Pomakidou S, Marmarinos C, Agrotou S, Moustogiannis A, Nikolopoulos A, et al. (2024) Wearable Motion Analysis in Sports: Advancing Biomechanical Insights Beyond the Laboratory. Chron Pain Manag 8: 165. DOI: 10.29011/2576-957X.100065

**Received Date:** 03 November 2024; **Accepted Date:** 11 November 2024; **Published Date:** 14 November 2024

**Abstract**

This study investigates the feasibility of estimating Ground Reaction Forces (GRFs) during various exercises using a wearable GPS sensor vest, combined with Artificial Neural Network (ANN) modelling. Traditional biomechanical assessments often rely on cumbersome optical motion capture systems and force platforms that limit real-world applicability. In contrast, this research leverages lightweight technology to gather kinematic data in natural training environments. A total of 6191 observations for the left leg and 5981 for the right leg were recorded, with the ANN trained to correlate GPS sensor data with GRFs. The results demonstrate predictive solid performance, evidenced by high $R^2$ scores and low Root Mean Squared Error (RMSE) in both the development and hold-out datasets. While the left leg's predictions were slightly less accurate than those for the right leg, the model proved effective overall in estimating GRFs. These findings suggest that wearable technology, when paired with ANN techniques, can provide reliable biomechanical insights outside controlled laboratory settings, paving the way for further research involving larger participant groups and diverse exercises. This study investigates the validity of using a wearable GPS sensor vest to estimate Ground Reaction Forces (GRFs) during various exercises, employing an Artificial Neural Network (ANN) model. Traditional methods for measuring GRFs, such as force platforms, are limited to controlled laboratory settings, hindering real-world applications in sports. Our research aims to bridge this gap by leveraging kinematic data obtained from the GPS vest, allowing for real-time monitoring in dynamic environments. A comprehensive experimental setup involving a professional athlete performing a series of exercises was established, utilizing both force platforms and wearable sensors. The ANN was trained to correlate the sensor data with GRFs, yielding promising results. Validation metrics, including $R^2$ and RMSE, demonstrated satisfactory accuracy of the model, particularly in predicting GRFs across different axes. The findings indicate that the proposed method can effectively estimate GRFs, providing valuable insights for performance optimization and injury prevention in sports. Future studies are recommended to expand the model's applicability across a broader range of athletes and exercise types.

## Introduction

Motion analysis is increasingly gaining interest in the scientific community, especially in supporting the medical and performance teams around professional athletes. Understanding and applying biomechanics in sports brings objectivity in areas where decisions were traditionally governed by personal experience and intuition [1].

Among the most popular and well-established tools employed in sports environments for biomechanical analyses are optical motion capture systems, whereby camera arrays track passive or active markers placed on specific anatomical positions of the body to provide a full-body capture. Despite been extensively used in research for sports science applications, optical systems have the insurmountable problem of being confined to indoor laboratory settings [2,3].

In consideration of the need to overcome set-up limitations and to be able to set up limitations and conduct real-life monitoring in the actual training and game environment, wearable technology is becoming more and more increasingly available. Elite athletes have been the early adopters of such technologies, but the niche segment is ever growing and today, several sports in national and international associations are using wearable sensors. Athletes, coaches, performance, and medical teams have access to information on range of motion, accelerations, impacts, or other indicators, such as biometric markers, which, if properly interpreted and assessed, can assist them in maximizing performance and minimizing injury risk for their athletes [4,5].

The increased availability of wearable movement sensors, their small and lightweight design, and the advantage of providing real-time feedback, contrary to motion capture or force plate systems, gives rise to the potential of an ever-increasing number of athletes to be monitored in their natural training and game environment [6,7]. Apart from physiological biometric characteristics, the possibility of monitoring the external biomechanical stresses is of immense value as it is the means to shift to the loads imposed on the body's soft tissues, further offering a more direct assessment of injury risks for the individual motor units.

Regarding injury risk, ground reaction forces (GRFs) are indispensable as they provide a measure of the external forces applied, further breaking down to different internal stresses on the hard and soft tissues of the body's construction. GRFs as the starting point of a series of internal organismic responses constituting the musculoskeletal adaptations [8,9]. In this respect, GRFs become a primary parameter of interest, whereby the external biomechanical loadings can be related to the responses of the tissue construction of the human body. These responses may be beneficial but may also significantly increase the risk for injury. The gold-standard measurement of GRFs is through the use of force platforms, which are nowadays highly accurate and can provide output for 3-axis force and momentum components. However, they have the limitation of being cumbersome and practically not applicable to real environment field measurements.

Hence, for the past few years, researchers have been investigating techniques to estimate GRFs using wearable sensors. Several published works employ methods based on biomechanical modelling [10]. The number of interacting factors and complexity of these models make it more difficult to depict the whole dynamics, thus giving rise to modelling errors.

On the other hand, artificial neural network (ANN) algorithms are emerging as an attractive alternative to unveiling the correlations accompanying such complex systems. ANNs have been widely adopted to successfully simulate the relationships between selected inputs and outputs in many studies of human locomotion [11]. There is no "golden rule" for defining a proper neural network. A trial-and-error approach is quite common to arrive at an adequate description of the underlying phenomena.

This study aims to assess the validity of a method to estimate GRFs during different exercises using a wearable GPS sensor vest. An ANN is defined and trained to depict the relationship between a component of acceleration and its corresponding component of the ground force, taking into consideration the interactions between the components on the different axes.

## Materials & Methods

### Experimental Set-Up

The gait and movement analysis laboratory of ELEPAP Athens has:

10 3D recording cameras (3D Vicon Cameras)

2 2D recording digital cameras (Pentax & Panasonic digital Cameras)

2 power recording force platforms (AMTI)

3 portable electromyographs (Noraxon 8 channel)

1 footprint device (Medicapture)

1 portable muscle strength meter (Hoogan)

1 adjustable clinical examination bed

5 computers

7 different types of software for analysis of the above data

Measurements that can be performed on a case-by-case basis are 3D Kinematic Analysis, 3D Kinetic Analysis, Muscle Strength Analysis, Walking Electromyogram, Footprint (static / equilibrium and dynamic), Clinical Examination, Equilibrium Analysis, etc.

**3D Kinematic Analysis**

Kinematic Analysis records the joints' angular track during movement on all three levels of the body. Furthermore, it records the spatio-temporal elements of movement, such as speed, distance, pacing pace, periods of support and swing, etc. It compares all joints, at each level for the right and left half, and at the same time compare them with the normal values.

**3D Kinetic Analysis**

Kinetic Analysis explains why the body moves this way. It analyzes the reaction forces from the ground to each joint at every level. In addition, it captures the torques applied to each joint, which results in the movement itself. Finally, it analyzes the power generation for each joint.

**Electromyographic Examination**

The electromyogram measures the electrical activity of muscles. It gives information about muscle activation during the execution of complex movements, and it is able to compare the right with the left half, at the same time simultaneously with the normal values.

**Equilibrium Analysis**

In Equilibrium Analysis, the body oscillation above the support base is evaluated. The pressure points and the magnitude of its deviation from the normal data are measured. The most valid tests are the conservation of balance with eyes open and closed. It can also assess whether there is an asymmetric charge between the lower extremities.

**Method followed**

The force plates were embedded in the laboratory floor. The athletes participating wore a vest consisting of GPS sensors and a gyroscope while performing a series of exercises. These sensors recorded a multi-dimensional input corresponds corresponding to the linear acceleration on the three axes of motion (x,y,z), three gyroscope measures, one for each axis (x,y,z), the speed and the instantaneous acceleration impulse. The output consists of the three-dimensional force components on the three spatial axes. Meanwhile the athletes were performing the exercises on the force plates measuring the GRFs.

Measurements from the GPS sensors were used as input data for the ANN, and the GRFs were the model's outputs. Linear interpolation was applied to the data recorded by the GPS sensors in order for the input data to match the 10-fold lower sampling frequency of the force plate output data.

**Experimental protocol**

1 healthy professional athlete voluntarily participated in this research. The athletes were instructed to perform a series of exercises. Those exercises derive from 10 simple movements, which were selected from the NSCA Basics of Strength and Conditioning Manual [12], based on the assumption that all complex movements are the algebraic summary of those simple ones. When jumps were included, the exercise was performed on the center of the force plate to ensure consistency of the measurements.

The exercises were the following:

**Exercise 1:** The athlete, while standing on one foot, pushed off at maximal capacity to achieve a maximal-height vertical jump. He landed on the same foot, step stepped forward onto the second force plate with the other foot, and then immediately maneuvered to the other side. The exercise was executed two times, once for each leg. Figure 1 shows a series of still images of the key events of exercise 1.


**Figure 1:** Series of still images of exercise 1.

**Exercise 2:** The athlete, while standing on both feet, pushed off at maximal capacity to achieve a maximal-height vertical jump. He landed on both feet and then stepped forward on the second force plate with one foot and immediately maneuverer to the other side direction. The exercise was executed two times for each direction.

**Exercise 3:** The athlete performed a rapid acceleration up to the center of the second force plate, where they abruptly made a sidestep-cutting manoeuvre with one leg stopping followed by sidestepping. The exercise was executed twice for each side.

**Exercise 4:** The athlete performed maximal acceleration efforts over the corridor of X m length where the force plates were embedded.


ISSN: 2576-957X

**Exercise 5:** The athlete performed maximal acceleration until they reached the second force plate, where they abruptly tried to decelerate as fast as possible.

**Artificial neural network**

Artificial neural networks consist of computational units that are interconnected to each other and distributed in layers. A feedforward network with backpropagation was utilized. The connections between units of continuous layers are weights. Input data is presented to the units of the first layer. From this layer, the data is forwarded to the units in the hidden layer while the data is forwarded to the units in the hidden layer while the data is forwarded to the units in the hidden layer, and the data is multiplied by the weight factor. In each receiving unit, the weighted data of all incoming connections is summed, and a bias term is added. Then, the summed input plus the bias term is processed by an activation function. This is the output value, which is then forwarded to the units of the next layer. By adjusting the weights, the network can be trained. In this study, it can find relationships between input and output patterns, which is the relationship between GPS sensor data and GRFs. To train a neural network, we provide data from both GRF measurements and GPS sensors for several conditions [13].

After the training is complete, the network can use one specific pattern. The power of an ANN is its ability to generalize `knowledge' obtained during training for a selected set of situations to new situations for which it has not been trained. The quality of the predictions of a network is influenced by of several factors: the number of units within the network, the pre-defined error within the output, and also the relative amount of knowledge within the training set. A network cannot be appropriately trained to map patterns when it does not contain enough units. When the level of the minimum error is set too high, the network will not converge enough to learn the mapping of the pattern. When the level is set too low, there is a risk of overtraining the network, thus obstructing the network from generalizing and predicting output signals for data it has not been trained with. In this study, both the number of units in the network and the number of iterations, which are directly related to the pre-defined error, were assessed in a pilot study by optimizing the quality of the predictions. The independent variable in this study was the amount of information provided to an ANN. In general, a network is strained and a data set encompassing a wider range of information will incorporate a better mapping of a relationship than a network trained with a narrower range of information [14-16].

**ANN Implementation**

The dataset had 6191 observations for the left leg and 5981 for the right leg. The datasets were partitioned into a development and a hold-out sample, respectively. The hold-out samples consisted of a random sample of 495 observations (circa 8%) for the left leg and 478 observations (circa 8%) for the right leg. For the development dataset, a 5cross-validation methodology was employed to get an unbiased estimate of model performance when making predictions on new data.

The ANN in this study was configured to model the relationship between training and testing data. Its flexible structure and many configurable internal parameters offered the additional value of capturing not only linear but also complex non-linear relationships. Calculations were carried out using Python (version 3.7). For the implementation, the NumPy [17], Pandas [18], Matplotlib [19], Sklearn [20], TensorFlow [21,22], and Keras [23] libraries were used from the Python environment.

An ANN architecture consisting of an input layer of 8 artificial neurons, 2 hidden layers of 32 neurons each, and an output layer, consisting of 3 neurons, was developed (Figure 2). To confront the regression problem and to avoid the output constraints of the sigmoidal activation function, a ReLU (Rectified Linear Units) activation function for the 2 hidden layers and a Linear activation function for the output layer were used. A ReLU activation function is a piecewise linear function that will output the input directly under the condition that it is positive or it will output zero otherwise. The aforementioned hyperparameters, as well as the choice of scalar, batch size, and number of epochs, were obtained via a 4:1 random sampling process on the development dataset into training and test datasets, with N=10 iterations for each combination of hyperparameters. The evaluation metric used , hence, to derive the optimum combination of hyperparameters and, hence, the optimum ANN architecture was the Mean Squared Error (MSE).

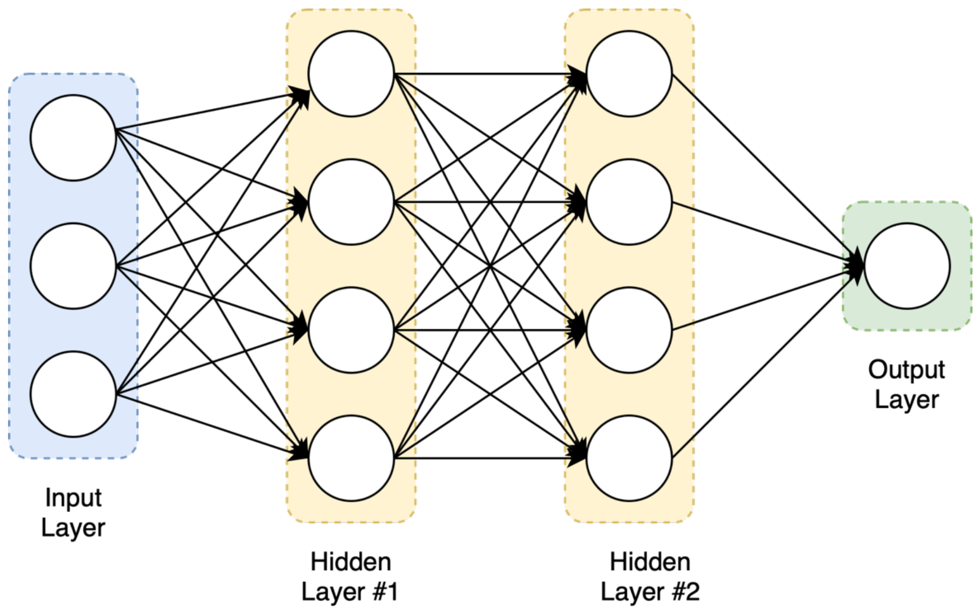


**Figure 2:** Artificial Neural Network with 2 hidden layers.

Figure 3 illustrates the phases of the ANN model implementation. The initial step of model execution involves the scaling of data collected for each repetition of each different exercise. This routine involves the linear interpolation of GPS data in order to match the dimensions of the force data frames.

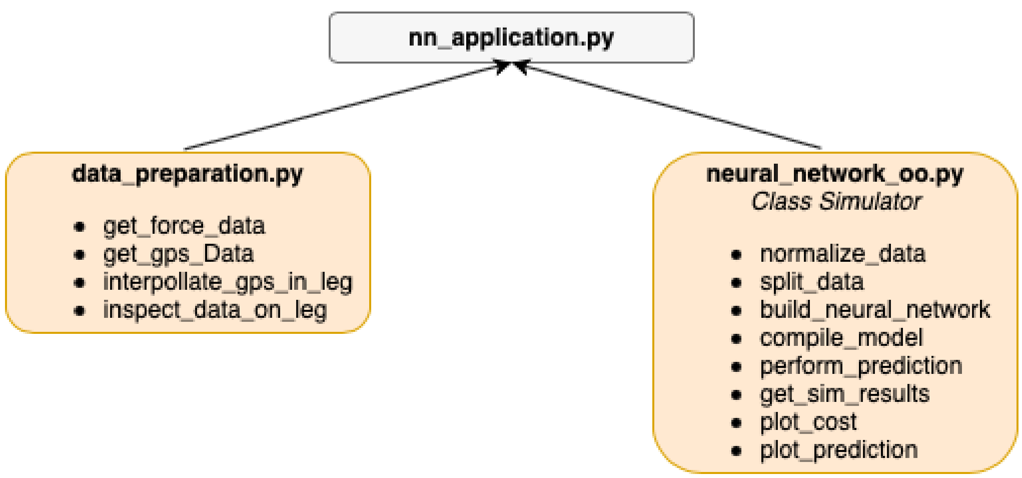


**Figure 3:** Data preparation and model development phases of the Artificial Neural Network (ANN) implementation.

Neurons have activation functions and are arranged in different horizontal layers, with multiple vertical layers possible. Within the hyperparameter grid search cross-validation optimization process, six processes were included in the sequence of ANN model construction: splitting the data into training and test datasets, scaling of input and output data, network training, network recollection, rescaling of input and output data and evaluating the model fit. These processes were repeated N=10 times for each parameter selection. Regarding the value of N, there is a trade-off between accuracy and computational complexity; i.e., as N increases, so does the accuracy of the described methodology, but so does the computational time need. To ascertain a more generalized indication of model performance, a sufficient number of trials was performed.

The feedforward ANN model built as part of this study falls into the category of supervised learning methodologies. Supervised learning refers to the fact that during the training process, the network is provided with data that hold both the input data (GPS sensor measurements) and the simultaneously recorded output signal (Force plate measurements). This way, the output generated by the network and the actual output can be compared. The network is trained via the backpropagation algorithm, which refers to the process by which the weight factors and bias terms are adjusted to map the predicted and actual output patterns. Initially, the weight and bias term are set to random values. A specific input shape of data that is propagated through the network will consequently generate a random output value. Subsequently, the error between the predicted output and the actual output is calculated. This error signal is transmitted from the output layer to each unit in the previous layer. Since each unit in the previous layer contributes only partly to the output signal, each unit also receives only a portion of the total error signal. This process continues for each layer until every unit has received its error signal. The weights and biases related to a unit are adjusted based on the error signals. Iteratively executing the cycle of forwarding an input signal and adjusting the weights and biases causes the network to converge; the error between the generated and actual output is then minimized. The optimizer used within the backpropagation algorithm in order to train the feed-forward ANN model is the Adam optimizer, an extension of stochastic gradient descent, and the loss function used was the MSE. The iterative process stops when the number of epochs is covered. The resulting number of optimum epochs of the hyperparameter grid search performed via random sampling of the development dataset was 500 epochs.

**Data analysis**

Experimental data across both legs for one athlete was used for training and validating the ANN. To evaluate the performance of the optimum ANN model, as derived through the grid search optimization process described above, a five-fold cross-validation process was employed on the development dataset. This approach involves randomly dividing the set of observations into k=5 groups, or folds, of approximately equal size. The first fold is treated as a validation set, and the method fits the remaining k − 1 folds (training set). The average validation scores (k validation folds) are saved. This procedure was executed 30 times, and for the ANN prediction performance to be quantified, numerous evaluation metrics were considered, such as Mean Absolute Error (MAE), Mean Absolute Percentage Error (MAPE), Root Mean Squared Error (RMSE) and R2, were used. For the purposes of this study, the R2 (which is scale independent) and RMSE (which is scale-dependent) metrics are utilized to depict the ANN's overall performance.

**Results**

The 3D kinetics data during the exercises were estimated using the ANN model. The predicted kinetics data are the spatial dimensions of the GRFs. The cost function of the ANN models trained on the development dataset and validated on the hold-out sample is depicted in Figures 4 and 5 for the left and right leg, respectively.

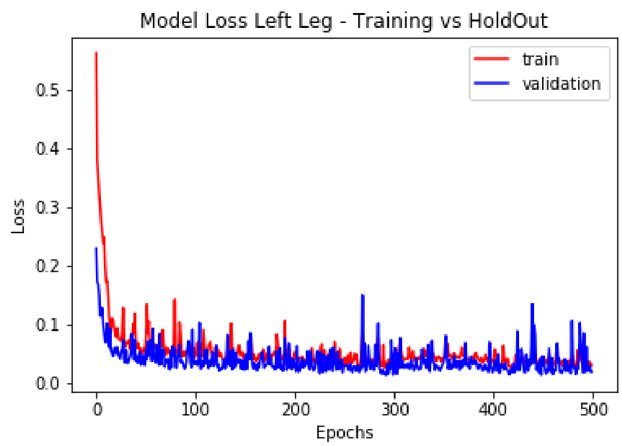


**Figure 4:** Cost function of the ANN model for an athlete on the left leg.

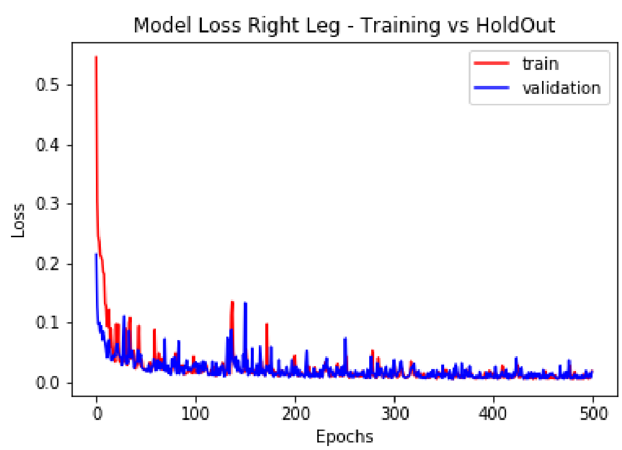


**Figure 5:** Cost function of the ANN model for an athlete on the right leg.

Figures 6 & 7 represent the actual/observed and predicted GRFs on the development dataset in the three spatial axes for the left and right leg, respectively.

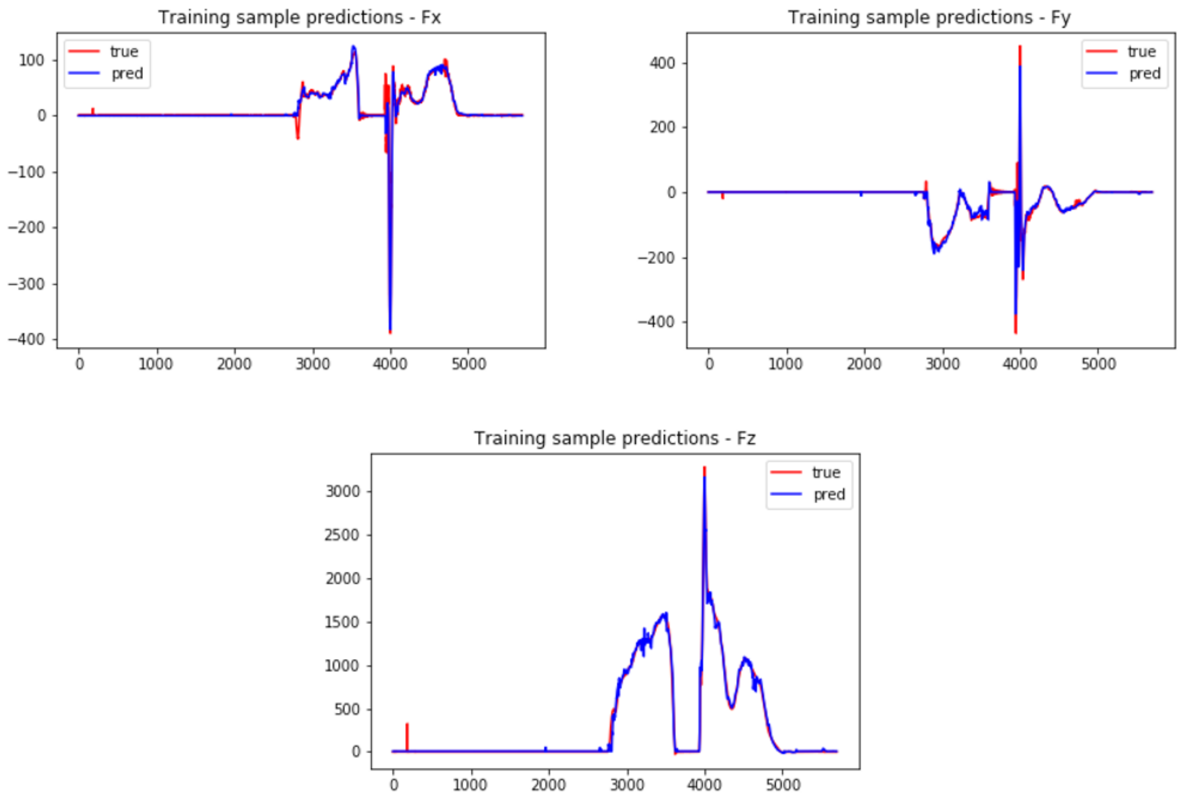


**Figure 6:** The measured (red) and predicted (blue) GRF in each of three axes, performed on the left leg for the development dataset.

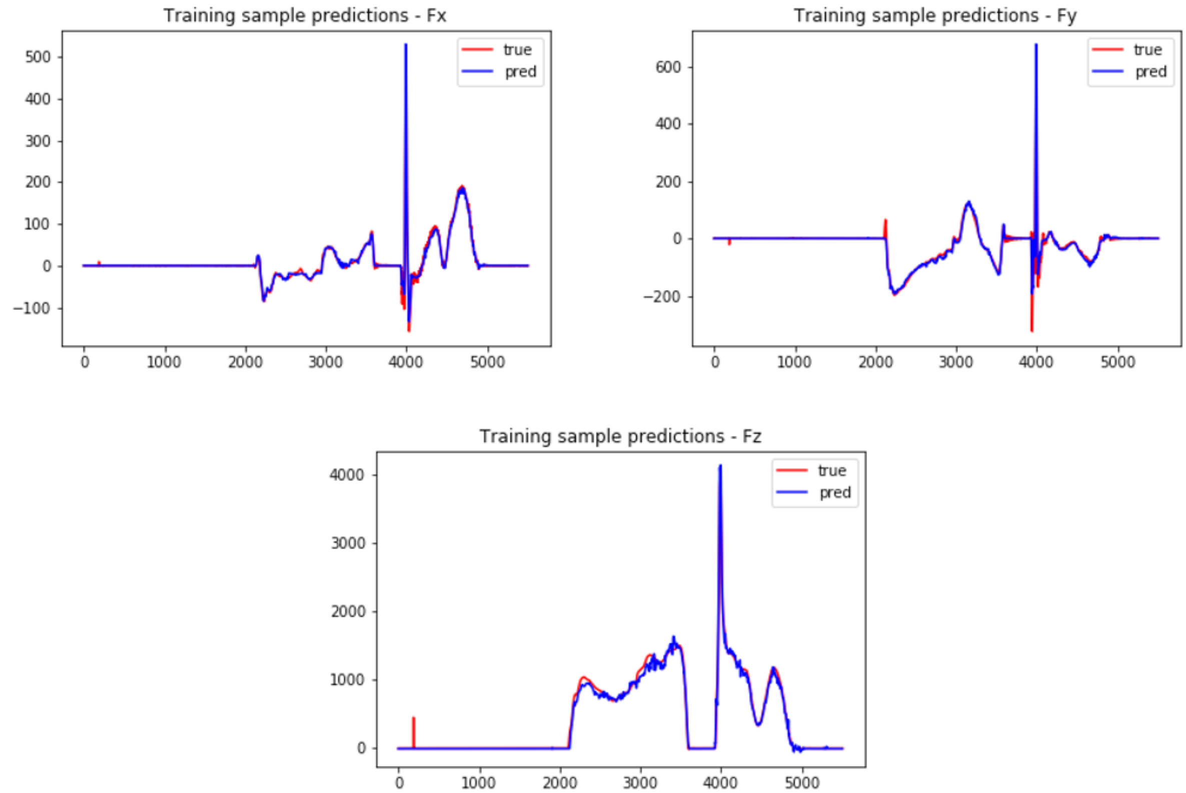


**Figure 7:** The measured (red) and predicted (blue) GRF in each of the three axes, performed on the right leg for the development dataset.

Numerical results for the R2 and RMSE scores across both models are presented in Tables 1 & 2 for the development dataset and in Tables 3 & 4 for the hold-out-sample. The R2 score, also known as the coefficient of determination, provides a statistical measure determining how close the fitted values are to the actual/target values. The RMSE is the standard deviation of the residuals (prediction errors). These measures give us an insight into the actual correlation between the predicted values and the actual values.

| **Left Leg** | $F_x$ | $F_y$ | $F_z$ |
|---|---|---|---|
| **5-fold CV average $R^2$ score performed for N=30 iterations** | 0.971 | 0.919 | 0.991 |
| **5-fold CV average RMSE score performed for N=30 iterations** | 5.902 | 13.102 | 51.259 |

**Table 1:** $R^2$ and RMSE scores of the development dataset for the GRF across the three axes of motion performed on the left leg.

| **Right Leg** | $F_x$ | $F_y$ | $F_z$ |
|---|---|---|---|
| **5-fold CV average $R^2$ score performed for N=30 iterations** | 0.987 | 0.976 | 0.995 |
| **5-fold CV average RMSE score performed for N=30 iterations** | 5.133 | 8.803 | 41.768 |

**Table 2:** $R^2$ and RMSE scores of the development dataset for the GRF across the three axes of motion performed on the right leg.

Tables 3 and 4 summarize the models' overall performance for the hold-out sample. In addition, Figures 8 and 9 represent the actual/observed and predicted GRFs on the hold-out sample in the three spatial axes for the left and right leg, respectively.

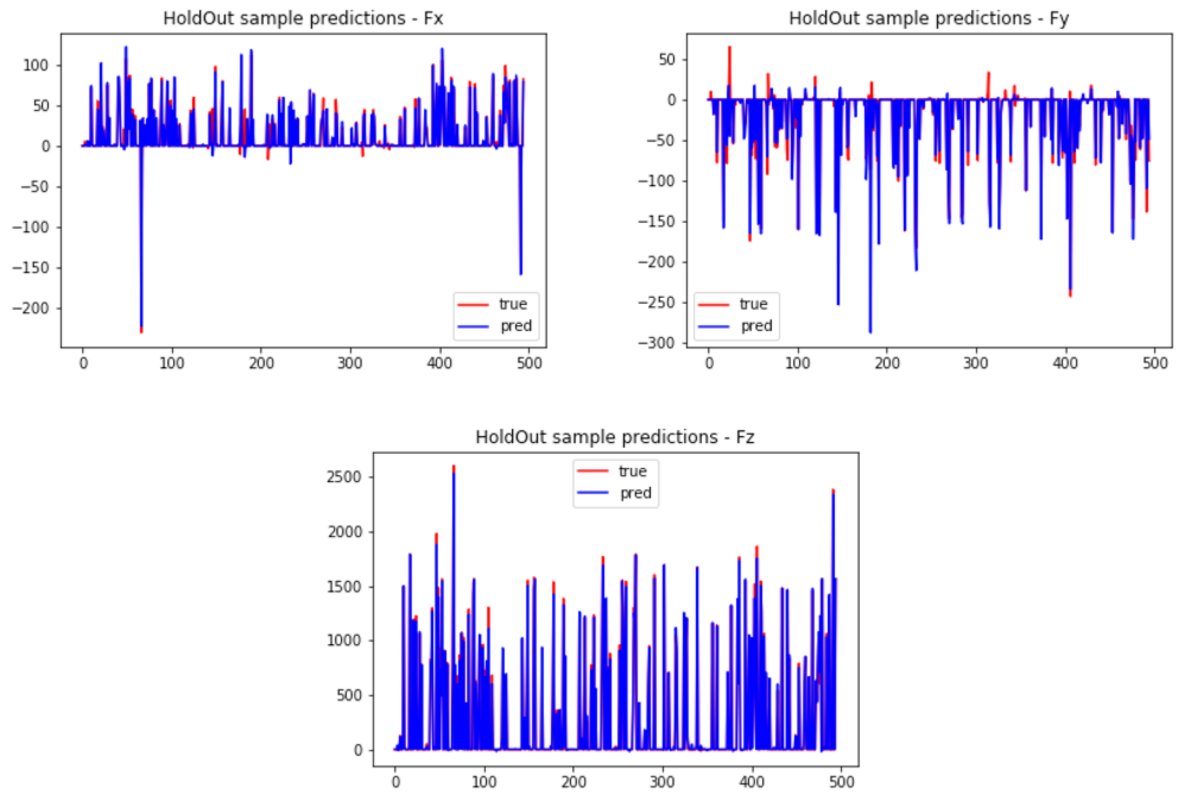


**Figure 8:** The measured (red) and predicted (blue) GRF in each of the three axes, performed on the left leg for the hold-out sample.

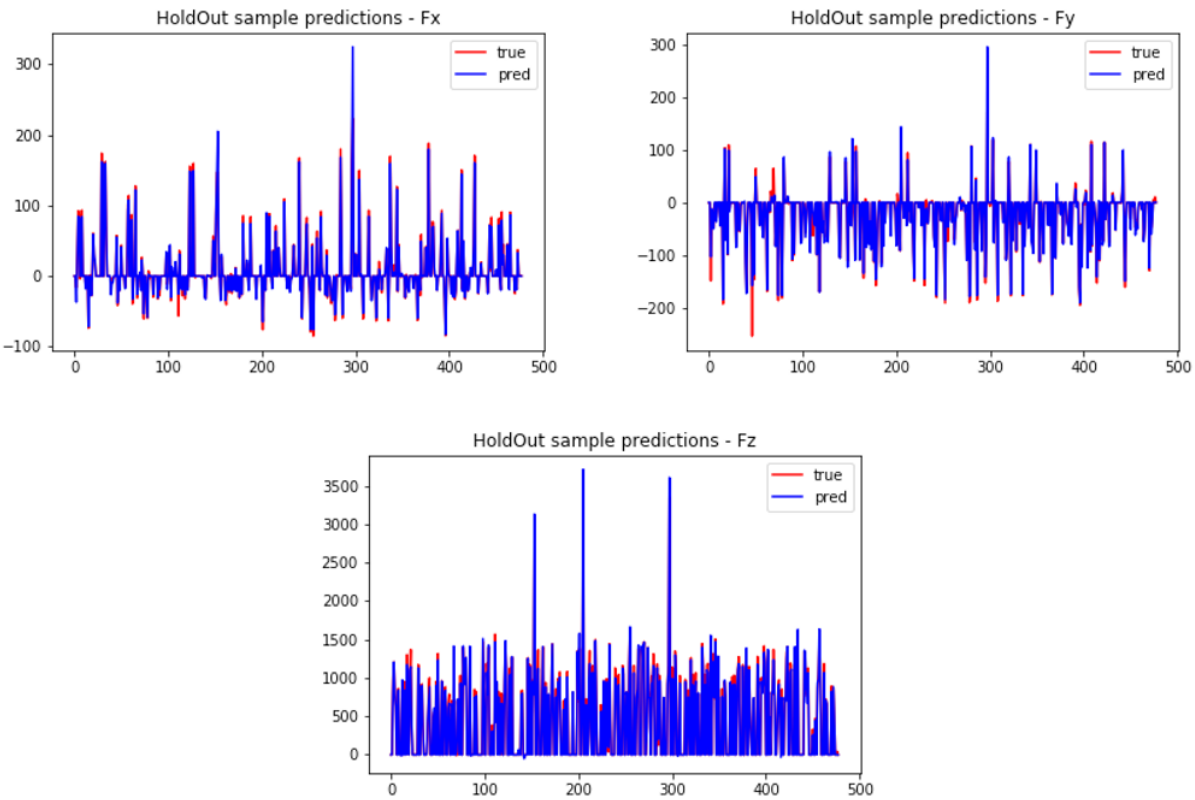


**Figure 9:** The measured (red) and predicted (blue) GRF in each of the three axes, performed on the right leg for the hold-out sample.

| **Left Leg** | $F_x$ | $F_y$ | $F_z$ |
|---|---|---|---|
| **$R^2$ on the hold-out sample** | 0.954 | 0.865 | 0.995 |
| **RMSE on the hold-out dataset** | 6.157 | 14.854 | 36.029 |

**Table 3:** $R^2$ and RMSE scores of the hold-out sample for the GRF across the three axes of motion performed on the left leg.

| **Right Leg** | $F_x$ | $F_y$ | $F_z$ |
|---|---|---|---|
| **$R^2$ on the hold-out sample** | 0.966 | 0.953 | 0.991 |
| **RMSE on the hold-out dataset** | 7.588 | 11.675 | 55.159 |

**Table 4:** $R^2$ and RMSE scores of the hold-out sample for the GRF across the three axes of motion performed on the right leg.

## Discussion

So, has our claim that we found a valid method to estimate GRFs during different exercises using a wearable GPS sensor vest been verified?

From the above results, we can make the following observations:

- From Figures 4 & 5, it can be verified that the training function and the validation loss functions (MSE) converge through time. This fact confirms that the model is accurate enough after completing the training process. It should be noted that the loss values of the left leg model, to the number of epochs utilized, appear to be higher and more volatile overall than the loss values of the right leg model.

- From Figures 6 & 7, we notice that the forces on all three axes have little difference from the actual measurements. This means that the estimation accuracy of the model is satisfactory for predicting the forces since the estimated ones mostly coincide with the actual measurements.
- From Tables 1, 2, 3 & 4, the R2 validation scores for the left leg were generally lower, and the RMSE scores were higher than the right leg across all axes, which agrees with the increased values and volatility of the left leg's corresponding cost function (Figures 4 & 5). However, predictions for the left leg are sufficiently good, with an overall high R2 (Tables 1 & 2) and a satisfactory fit to the observed values (Figure 6). These results confirm that the ANN models developed in this study can reflect the actual data measured by the force plate, namely the patterns between GPS sensors and GRFs.

This work shows that, indeed, GRFs can be estimated using only the measurements supplied by a tracking vest. GRFs are a reliable source of data with the lowest calculation error, making these data ideal for motion analysis. However, they can only be acquired using a force platform, thereby being accompanied by space constraints. Such a limitation makes it impossible to conduct motion analyses outside of the lab. In this study, an artificial neural network is applied to predict GRFs during dynamic conditions using kinematic data obtained from a vest consisting of GPS sensors. ANN is one of the artificial intelligence techniques usually used when interrelationships between data are non-linear and complex.

To further analyze the relationship between the actual measured and the model estimates of GRFs, functional measures based on the R2 and RMSE scores in predicting common GRF variables across the dataset were also employed. The employed ANN led to efficient estimations of the forces across all tested exercises and for both legs. The z-axis, followed by the x-axis GRF, showed the highest accuracy across both models employed. The accuracy of both models on the y-axis was slightly lower. Moreover, the predictive performance, as demonstrated by the average cross-validation $R^2$ and RMSE scores, was generally higher across axes for the right leg.

Comparing the results of this study to earlier literature could not be straightforward; most previous studies focused on static postures and gait. One of the first works involving ANNs is the one by Leporace et al. [24], where two models were compared based on ANN to estimate GRFs while walking Then error analysis suggested that both the models adequately predicted the GRF on vertical, mediolateral, and antero-posterior projections. The size of the sample used to train the model was crucial to reaching an accurate result. However, the size of the sample was rather small in this study. However, accurate predictions were acquired for both models and across axes.

Predicting GRFs from GPS sensor data constitutes a multi-output regression problem with continuous features and target variables. Neural network models have the benefit of learning a continuous function that can model a relationship between changes in input and output in a more intuitive way compared to other machine learning methodologies, both from an implementation standpoint (within Python) and from a methodological standpoint [25,26].

Firstly, the convergence of the training and validation loss functions (MSE) for both legs indicates that the artificial neural network (ANN) model is effectively learning the underlying relationships between the input data from the GPS sensors and the output data from the ground reaction forces (GRFs). This convergence suggests that the model has achieved a satisfactory level of accuracy, which is crucial for its application in real-world sports contexts where precise measurements of force are necessary for performance analysis and injury prevention. However, it is worth noting that the volatility of the loss values for the left leg compared to the right leg might imply inherent differences in biomechanics or sensor performance that warrant further investigation. Moreover, the close alignment of predicted GRFs with actual measurements emphasizes the model's reliability. This is particularly significant in the context of sports science, where traditional methods for measuring GRFs often require cumbersome laboratory setups that restrict athletes to controlled environments. The ability to estimate GRFs accurately through wearable technology could revolutionize how athletes train and compete, as it allows for continuous monitoring and real-time feedback in natural settings. The findings confirm that the ANN can serve as a viable alternative to conventional methods, potentially enhancing the practicality of biomechanical analysis in sports.

The observed differences in $R^2$ and RMSE scores between the left and right legs also highlight an important consideration for future applications of this technology. The lower $R^2$ values and higher RMSE scores for the left leg may reflect biomechanical asymmetries or differences in athletic performance that could be further explored. Understanding these discrepancies could lead to more personalized training regimens and injury prevention strategies tailored to individual athletes. In addition, the successful application of ANNs in this study aligns with emerging trends in sports science that leverage machine learning to analyze complex data relationships. This points to a broader potential for integrating artificial intelligence into sports analytics, extending beyond GRF estimation to encompass various performance metrics and physiological indicators. Future research could explore the integration of additional biometric data, such as heart rate variability or muscle activation patterns, to enhance the model's predictive capabilities further [27,28].

Finally, the study's limitations regarding the sample size and the diversity of exercises performed should be addressed in future work. Expanding the dataset to include a broader range of athletes, exercises, and conditions will enhance the generalizability of the ANN model. This will not only validate the findings but also refine the model to account for variations in movement patterns across different sports and populations.

In conclusion, the promising results of this study underscore the potential of wearable technology and artificial intelligence in advancing the field of sports biomechanics. By facilitating real-time monitoring of GRFs, this innovative approach could lead to significant improvements in athlete performance and injury prevention strategies. Future research endeavors should focus on validating and expanding the model to harness its full potential in diverse athletic contexts [29,30].

## Conclusion and Future Work

Future work may include as applying the proposed model to more athletes and for more exercises performed further to verify the accuracy of the model's predictive capabilities and extend the model's scope. Indeed, the absence of a multitude of data sources is this study's most significant limitation as far as its generalization capabilities are concerned. All things considered, the ANN model developed in this study appears to be effective as a mapping tool for estimating GRFs utilizing only vest GPS data sources.

## References


1. Gabbett TJ (2016) The training-injury prevention paradox: should athletes be training smarter and harder? Br J Sports Med 50: 273-280.
2. Pueo B, Jimenez-Olmedo JM (2017) Application of motion capture technology for sport performance analysis. RETOS. Nuevas Tendencias en Educación Física, Deporte y Recreación 241-247.
3. Adesida Y, Papi E, McGregor AH (2019) Exploring the Role of Wearable Technology in Sport Kinematics and Kinetics: A Systematic Review. Sensors (Basel) 19: 1597.
4. Li RT, Kling SR, Salata MJ, Cupp SA, Sheehan J, et al. (2016) Wearable Performance Devices in Sports Medicine. Sports Health 8: 74-78.
5. Vanrenterghem J, Nedergaard NJ, Robinson MA, Drust B (2017) Training load monitoring in team sports: a novel framework separating physiological and biomechanical load-adaptation pathways. Sports Med 47: 2135-2142.
6. Kibler WB, Chandler TJ, Stracener ES (1992) Musculoskeletal adaptations and injuries due to overtraining. Exerc Sport Sci Rev 20: 99-126.
7. Ancillao A, Tedesco S, Barton J, O'Flynn B (2018) Indirect Measurement of Ground Reaction Forces and Moments by Means of Wearable Inertial Sensors: A Systematic Review. Sensors (Basel) 18: 2564.
8. Luh JJ, Chang GC, Cheng CK, Lai JS, Kuo TS (1999) Isokinetic elbow joint torques estimation from surface EMG and joint kinematic data: using an artificial neural network model. J Electromyogr Kinesiol 9: 173-183.
9. Chau T (2001) A review of analytical techniques for gait data. Part 2: neural network and wavelet methods. Gait Posture 13: 102-120.
10. Wang L, Buchanan TS (2002) Prediction of joint moments using a neural network model of muscle activations from EMG signals. IEEE Transactions on Neural Systems and Rehabilitation Engineering 10: 30-37.
11. Begg R, Kamruzzaman J (2005) A machine learning approach for automated recognition of movement patterns using basic, kinetic and kinematic gait data. J Biomech 38: 401-408.
12. Schöllhorn WI (2004) Applications of artificial neural nets in clinical biomechanics. Clin Biomech (Bristol, Avon) 19: 876-898.
13. Holzreiter S (2005) Autolabeling 3D tracks using neural networks. Clin Biomech (Bristol, Avon) 20: 1-8.
14. Hahn ME (2007) Feasibility of estimating isokinetic knee torque using a neural network model. J Biomech 40: 1107-1114.
15. Stetter BJ, Ringhof S, Krafft FC, Sell S, Stein T (2019) Estimation of knee joint forces in sport movements using wearable sensors and machine learning. Sensors 19: 3690.
16. Sands AW, Wurth JJ, Hewit KJ (2012) The National Strength and Conditioning Association's (NSCA) Basics Of Strength And Conditioning Manual.
17. Oh SE, Choi A, Mun JH (2013) Prediction of ground reaction forces during gait based on kinematics and a neural network model. J Biomech 46: 2372-2380.
18. Choi A, Lee JM, Mun JH (2013) Ground reaction forces predicted by using artificial neural network during asymmetric movements. International Journal of Precision Engineering and Manufacturing 14: 475-483.
19. Savelberg HH, de Lange ALH (1999) Assessment of the horizontal, fore-aft component of the ground reaction force from insole pressure patterns by using artificial neural networks. Clin Biomech 14: 585-592.
20. Koeppe A, Bamer F, Markert B (2019) An efficient monte carlo strategy for elasto-plastic structures based on recurrent neural networks. Acta Mechan 230: 3279-3293.
21. NumPy: The fundamental package for scientific computing with Python.
22. Pandas: Python Data Analysis Data.
23. Matplotlib: Visualization with Python.
24. Scikit-Learn: Machine Learning in Python.
25. TensorFlow: An end-to-end open source machine learning platform.
26. Abadi M, Agarwal A, Barham P, Brevdo E, Chen Z, et al. (2015) TensorFlow: Large-scale Machine Learning on Heterogeneous Systems.
27. Keras: Keras is a deep learning API written in Python, running on top of the machine learning platform TensorFlow.
28. Leporace G, Batista LA, Metsavaht L, Nadal J (2015) Residual analysis of ground reaction forces simulation during gait using neural networks with different configurations. Annu Int Conf IEEE Eng Med Biol Soc 2015: 2812-2815.
29. Xu D, Shi Y, Tsang IW, Ong YS, Gong C, et al. (2019) Survey on multi-output learning. IEEE Transactions on Neural Networks and Learning Systems 31: 2409-2429.
30. Antanasijevic D, Pocajt V, Peric-Grujic A, Ristic M (2018) Multiple-input–multiple-output general regression neural networks model for the simultaneous estimation of traffic-related air pollutant emissions. Atmospheric Pollution Research.